Acta Cryst C STRUCTURAL CHEMISTRY
ISSN 2053-2296

Regioselective synthesis and characterization of monovanadium-substituted β-octamolybdate $[VMo_7O_{26}]^{5-}$

Lukáš Krivosudský,[a,b] Alexander Roller[c] and Annette Rompel[a]*

[a]Universität Wien, Fakultät für Chemie, Institut für Biophysikalische Chemie, Althanstrasse 14, Wien 1090, Austria, [b]Comenius University in Bratislava, Faculty of Natural Sciences, Department of Inorganic Chemistry, Ilkovičova 6, 842 15 Bratislava, Slovakia, and [c]Universität Wien, Fakultät für Chemie, Zentrum für Röntgenstrukturanalyse, Währinger Strasse 42, 1090 Wien, Austria. *Correspondence e-mail: annette.rompel@univie.ac.at

Received 14 March 2019
Accepted 2 May 2019

Edited by A. R. Kennedy, University of Strathclyde, Scotland

Keywords: polyoxometalate; POM; octamolybdate; vanadium; ^{51}V NMR spectroscopy; crystal structure.

CCDC reference: 1898165

Supporting information: this article has supporting information at journals.iucr.org/c

The monovanadium-substituted polyoxometalate anion $[VMo_7O_{26}]^{5-}$, exhibiting a β-octamolybdate archetype structure, was selectively prepared as pentapotassium [hexaikosaoxido(heptamolybdenumvanadium)]ate hexahydrate, $K_5[VMo_7O_{26}]\cdot 6H_2O$ (**VMo$_7$**), by oxidation of a reduced vanadomolybdate solution with hydrogen peroxide in a fast one-pot approach. X-ray structure analysis revealed that the V atom occupies a single position in the cluster that differs from the other positions by the presence of one doubly-bonded O atom instead of two terminal oxide ligands in all other positions. The composition and structure of **VMo$_7$** was also confirmed by elemental analyses and IR spectroscopy. The selectivity of the synthesis was inspected by a ^{51}V NMR investigation which showed that this species bound about 95% of V^V in the crystallization solution. Upon dissolution of **VMo$_7$** in aqueous solution, the $[VMo_7O_{26}]^{5-}$ anion is substantially decomposed, mostly into $[VMo_5O_{19}]^{3-}$, α-$[VMo_7O_{26}]^{4-}$ and $[V_2Mo_4O_{19}]^{4-}$, depending on the pH.

1. Introduction

Polyoxometalates (POMs) of W, Mo and V represent an important group of inorganic metal–oxide clusters (Pope, 1983) whose structural variability gives rise to an exceptionally wide range of applications in catalysis (Wang & Yang, 2015), magnetism (Clemente-Juan *et al.*, 2012), redox processes (Gumerova & Rompel, 2018) and materials chemistry (Song & Tsunashima, 2012), as well as in biological chemistry (Bijelic & Rompel, 2015, 2017; Molitor *et al.*, 2017; Fu *et al.*, 2015; Bijelic *et al.*, 2018, 2019). Particularly interesting are photoactive POMs with applications in water splitting, the photooxidation of organic pollutants, photoreductive CO_2 activation and H_2 generation (Streb *et al.*, 2019). Vanadium-containing POMs are a promising subgroup of photocatalysts. A V^V centre acts as a more efficient light absorber in comparison to Mo^{VI}/W^{VI}; moreover, it may easily promote a photoredox reaction *via* its photoreduction to a V^{IV} species. Substitution of some Mo or W atoms in molybdates and tungstates may therefore lead to enhanced photocatalytic properties (Streb, 2012). Substitution of one Mo atom in a Linqvist-type hexamolybdate, $[Mo_6O_{19}]^{2-}$, by vanadium leads to enhanced photocatalytic degradation of a model organic dye under both aerobic and anaerobic conditions caused by a low-energy O→V LMCT (ligand-to-metal charge transfer) transition in $[VMo_5O_{19}]^{3-}$ (Tucher *et al.*, 2012). However, the controlled synthesis of mixed vanadomolybdates and vanadotungstates remains a serious challenge. Simple mixing of addenda-atom

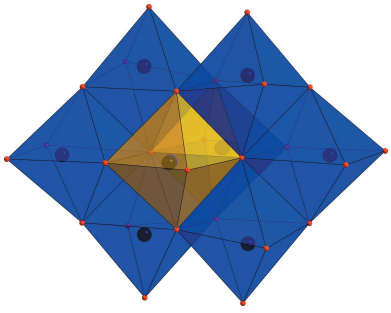

precursors leads to a complicated equilibria of several species (Pope, 1983; Howarth *et al.*, 1991). The β-octamolybdate structure $[Mo_8O_{26}]^{4-}$ (Fig. 1) is one of the main components in $H^+/OH^-/MoO_4^{2-}$ systems under acidic conditions, yet only the disubstituted vanadium derivative $[V_2Mo_6O_{26}]^{6-}$ is commonly known in the literature and has been structurally characterized (Nenner, 1985; Fei *et al.*, 2015; Li *et al.*, 2011). The two V atoms occupy chemically equivalent positions, denoted Mo_C. Very recently, a monovanadium-substituted derivative was prepared as $H_4K_2Na_2(H_2O)_4(C_{12}H_{12}N_4O_2)[VMo_7O_{26}]\cdot10H_2O$ (Zhao *et al.*, 2018). In this case, the V atom was claimed to be statistically distributed in all positions of the parent β-octamolybdate anion.

In the current work, we present a regioselective synthesis of a new isomer of $[VMo_7O_{26}]^{5-}$ in which the V atom occupies only Mo_C positions of the parent β-octamolybdate structure. The regioselectivity was achieved by controlled stepwise synthesis *via* vanadium peroxido complexes as precursors. The peroxide-mediated synthesis route (Schwendt *et al.*, 2016) has already been successfully utilized for the synthesis of several polyoxometalates, such as $[H_xV_{10}O_{28}]^{(6-x)-}$ (Jahr *et al.*, 1963; Nakamura & Ozeki, 2001), $[H_xPV_{14}O_{42}]^{(9-x)-}$, Keggin structures $[H_{3+x}PMo_{12-x}V_xO_{40}]$, and Wells–Dawson structures $[H_{6+x}P_2Mo_{18-x}V_xO_{62}]$ (Odyakov *et al.*, 2015) and $[V_{12}O_{30}F_4(H_2O)_2]^{4-}$ (Krivosudský *et al.*, 2014).

2. Experimental

All chemicals were purchased from Sigma–Aldrich (Austria) and used as received.

2.1. Synthesis and crystallization

For the preparation of $K_5[VMo_7O_{26}]\cdot6H_2O$ (**VMo$_7$**), K_2MoO_4 (1.67 g, 7 mmol) and $VOSO_4\cdot nH_2O$ (0.2 g, 1.22 mmol) were dissolved in distilled water (40 ml) by heating. HCl (0.7 ml of a 37% *w*/*w* solution) was added. When the temperature reached 80 °C, H_2O_2 (0.1 ml of a 30% *w*/*w* solution, 1 mmol) was added and the colour of the solution changed immediately from dark violet to orange. The solution was boiled for 1 min and the pH of the still hot solution was adjusted to 3.1 with 50% KOH solution. The clear-yellow solution was left to crystallize at 18 °C. Yellow block-shaped crystals were filtered off after 2 d, washed with water and ethanol and air-dried (yield 0.47 g, 33%, based on Mo). Elemental analysis (%) for $K_5Mo_7VO_{32}H_{12}$ (calculated): K 14.0 (13.6), Mo 46.6 (46.6), V 3.43 (3.53).

2.2. Elemental analysis

Elemental analyses were performed in aqueous solutions containing 2% HNO_3 using inductively coupled plasma mass spectrometry (PerkinElmer Elan 6000 ICP MS) for Mo and V, and atomic absorption spectroscopy (PerkinElmer 1100 Flame AAS) for K. Standards were prepared from single-element standard solutions of concentration 1000 mg l^{-1} (Merck, Ultra Scientific and Analytika Prague).

Table 1
Experimental details.

Crystal data	
Chemical formula	$K_5[VMo_7O_{26}]\cdot6H_2O$
M_r	1442.12
Crystal system, space group	Monoclinic, *C*2/*c*
Temperature (K)	143
a, *b*, *c* (Å)	12.9356 (10), 16.1978 (10), 13.8618 (9)
β (°)	90.962 (4)
V (Å^3)	2904.0 (3)
Z	4
Radiation type	Mo $K\alpha$
μ (mm^{-1})	4.06
Crystal size (mm)	0.1 × 0.1 × 0.1
Data collection	
Diffractometer	Bruker D8 Venture
Absorption correction	Multi-scan (*SADABS*; Bruker, 2016)
T_{min}, T_{max}	0.512, 0.564
No. of measured, independent and observed [$I > 2\sigma(I)$] reflections	80344, 4259, 4028
R_{int}	0.057
(sin $\theta/\lambda)_{max}$ (Å^{-1})	0.705
Refinement	
$R[F^2 > 2\sigma(F^2)]$, $wR(F^2)$, *S*	0.027, 0.059, 1.26
No. of reflections	4259
No. of parameters	235
No. of restraints	37
H-atom treatment	H-atom parameters not defined
$\Delta\rho_{max}$, $\Delta\rho_{min}$ (e Å^{-3})	0.64, −0.74

Computer programs: *APEX3* (Bruker, 2018), *SAINT* (Bruker, 2016), *SHELXS97* (Sheldrick, 2008), *SHELXL2018* (Sheldrick, 2015), *OLEX2* (Dolomanov *et al.*, 2009), *DIAMOND* (Brandenburg, 2006), *PLATON* (Spek, 2009) and *ShelXle* (Hübschle, *et al.*, 2011).

2.3. IR spectroscopy

VMo$_7$ was identified by IR measurement on a Bruker Vertex70 IR Spectrometer equipped with a single reflection diamond-ATR (attenuated total reflectance) unit in the range 4000–100 cm^{-1}.

2.4. ^{51}V NMR spectroscopy

^{51}V nuclear magnetic resonance spectroscopy measurements of aqueous solutions (with 10% of D_2O used for locking, at 20 °C) were taken on a Bruker AV II+ 500 MHz instrument operating at 131.60 MHz for the ^{51}V nucleus (2000 scans, accumulation time 0.05 s, relaxation delay 0.01 s). Chemical shift values are given with reference to $VOCl_3$ (0 ppm) as the standard.

2.5. Refinement

Crystal data, data collection, structure refinement and software details are summarized in Table 1. No H atoms were inserted on the free water O atoms due to the disorder and instability of the model. In the case of the disordered groups, one bond was added to the connectivity array (O15*S*—K3). The disordered Mo4*A*/V4 atoms occupying the same position of the POM anion were treated with half occupancies. The O atoms of the solvent molecules (O16*S*, O17*S*, O18*S* and O19*S*) and the partially occupied K3 and K4 atoms and their corre-

sponding U_{ij} components are of low quality and were forced by the restrained ISOR to affect the standard deviation and approximate the U_{ij} components to isotropic behaviour.

3. Results and discussion

Upon reaction of the initial $H_xVO_4^{(3-x)-}$ and $H_xMoO_4^{(2-x)-}$ precursors and adjustment of the pH to a certain value, complicated reaction mixtures with several equilibrated species are formed (Howarth *et al.*, 1991). It was therefore necessary to choose a different synthesis approach that would favour the formation of $[VMo_7O_{26}]^{5-}$. We employed a V^{IV} precursor ($VOSO_4$) that forms with molybdate mixed-valence polynuclear deep-blue vanadomolybdates at pH ≃1.5 (Müller *et al.*, 2005; Botar *et al.*, 2005). Subsequent addition of hydrogen peroxide resulted in an orange solution formed by immediate oxidation with vanadium peroxido complexes (Schwendt *et al.*, 2016). The crucial point of the synthesis was the adjustment of the pH of the hot solution to 3.1. This value represents a region where the β-octamolybdate anion $[Mo_8O_{26}]^{4-}$ is the main species present in the simple molybdate solutions at c_{Mo} = 0.1 mol dm^{-3} (Ozeki *et al.*, 1988). We also obtained different products from solutions with the pH range 1.5–7.0; however, IR and ICP–MS analyses indicated that the products are mixtures and **VMo$_7$** can only be obtained as a pure product in the pH range 2.8–3.5. Adjustment of the pH of the cooled solution leads to the formation of precipitates and an obvious reduction of vanadium (formation of a green solution).

The asymmetric unit of **VMo$_7$** contains one half of the $[VMo_7O_{26}]^{5-}$ POM anion lying on a centre of symmetry (Fig. 2). The K^+ cations which compensate the charge of the anion occupy four positions, one of them at full occupancy (K2) and one disordered over two positions (K3 and K4). The K1 atom is coordinated by two $[VMo_7O_{26}]^{5-}$ anions in an interesting fashion, forming an irregular twisted antiprismatic coordination polyhedron, with K—O distances in the range 2.703 (3)–2.767 (3) Å (Fig. 3) and without the participation of water molecules. The two square bases formed by oxido ligands O1, O2, O3 and O4 are twisted by approximately 10–13°. The $[VMo_7O_{26}]^{5-}$ anion adopts the expected β-con-

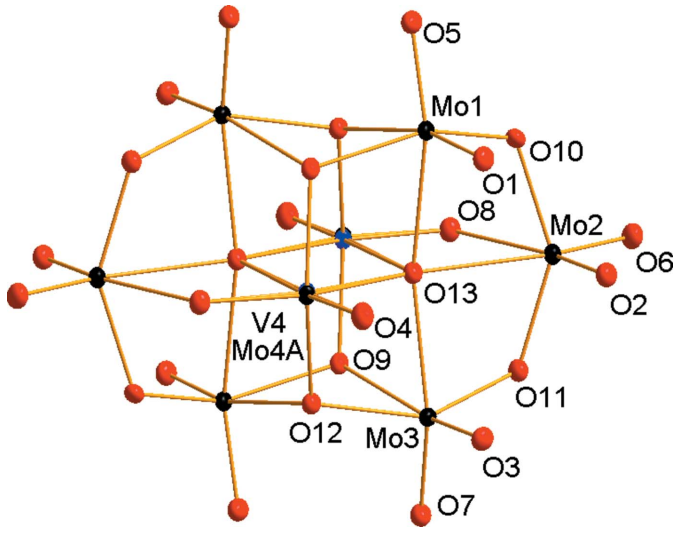

Figure 2
The molecular structure of $[VMo_7O_{26}]^{5-}$ in **VMo$_7$**, showing the atom-labelling scheme. Displacement ellipsoids are shown at the 50% probability level. Colour code: Mo black, V blue and O red.

formation (compare Figs. 1 and 2). The centrosymmetric anion was firstly refined as a pure $[Mo_8O_{26}]^{4-}$ cluster for localization of the V atoms. While the Mo_A and Mo_B positions showed initial occupancies very close to 1 (≃0.96), significantly lower occupancies of the Mo atoms at the Mo_C positions indicated the presence of V atoms which are equally distributed in both symmetrically equivalent positions. The positioning of the V atoms at 0.5 occupancies in the Mo_C positions led to a significant improvement of the model. Moreover, it can be seen from Fig. 1 that the Mo_C atoms differ significantly from the Mo_A and Mo_B atoms in the replacement of one Mo═O bond by a bridging Mo—O bond. Therefore, we consider it reasonable that the V atom occupies preferably position Mo_C which is not only crystallographically, but also chemically, markedly non-equivalent to the other positions in the octametalate. In this context, we should note for the structure of $H_4K_2Na_2(H_2O)_4(C_{12}H_{12}N_4O_2)[VMo_7O_{26}]\cdot10H_2O$ (Zhao *et al.*, 2018) that the displacement ellipsoids at the Mo_C positions are

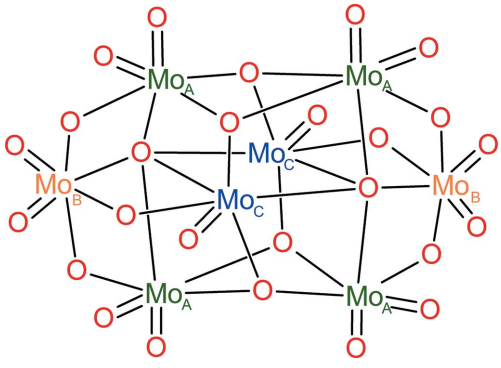

Figure 1
Schematic representation of the structure of the β-octamolybdate anion $[Mo_8O_{26}]^{4-}$. Chemically non-equivalent Mo atoms are shown in different colours: Mo_A green, Mo_B orange, Mo_C blue and O red.

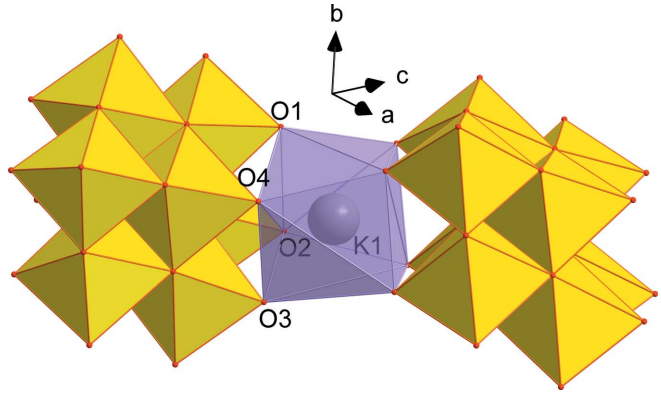

Figure 3
The coordination of the potassium cation K1 by two $[VMo_7O_{26}]^{5-}$ ligands. Colour code: {Mo/VO$_6$} yellow octahedra and {KO$_8$} violet distorted square antiprism.

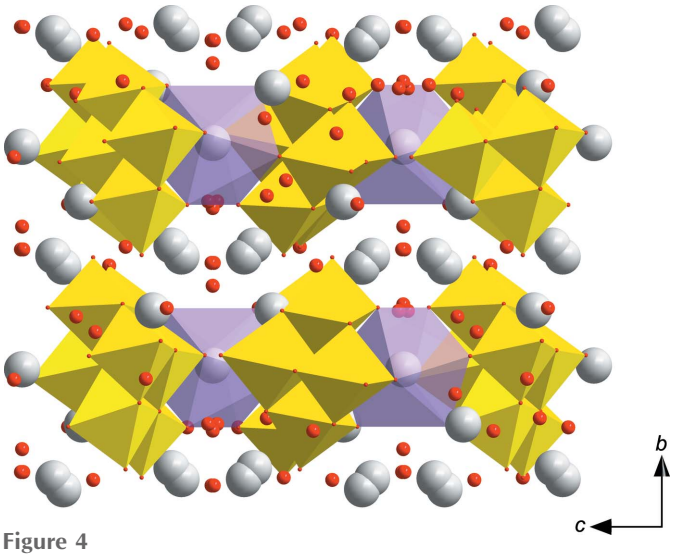

Figure 4
The crystal packing in **VMo$_7$**, viewed along the *a* axis. Colour code: {Mo/VO$_6$} yellow octahedra and {KO$_8$} violet distorted square antiprism. H atoms of water molecules have been omitted for clarity.

approximately twice as large as the ellipsoids of the Mo$_A$ and Mo$_B$ atoms, indicating that the V atom occupies preferably this position also in this structure, although the model was constrained with a statistical distribution of the V atoms throughout the anion. However, the selectivity of vanadium substitution is not known and the existence of such a species might be theoretically possible despite the fact that it was not predicted by speciation (Howarth *et al.*, 1991). $[VMo_7O_{26}]^{5-}$ consists of eight {Mo/VO$_6$} face- and edge-sharing octahedra. Except for atoms V4/Mo4*A*, all other Mo atoms are coordinated by two terminal oxido ligands, with shorter Mo═O double bonds in the range 1.601 (5)–1.726 (3) Å, and bridging oxide ligands exhibiting longer bond distances of up to 2.430 (2) Å for the Mo2—O13 bond incorporating the pentacoordinated O atom (see the supporting information for

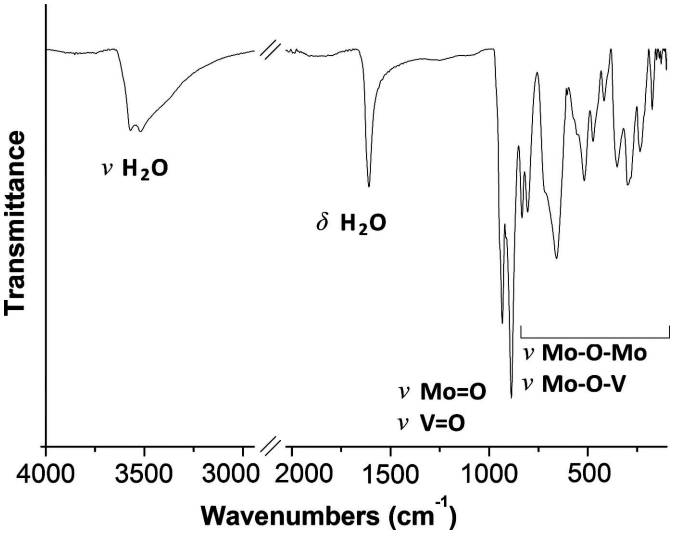

Figure 5
The IR spectrum of **VMo$_7$** in the region 4000–100 cm^{-1}.

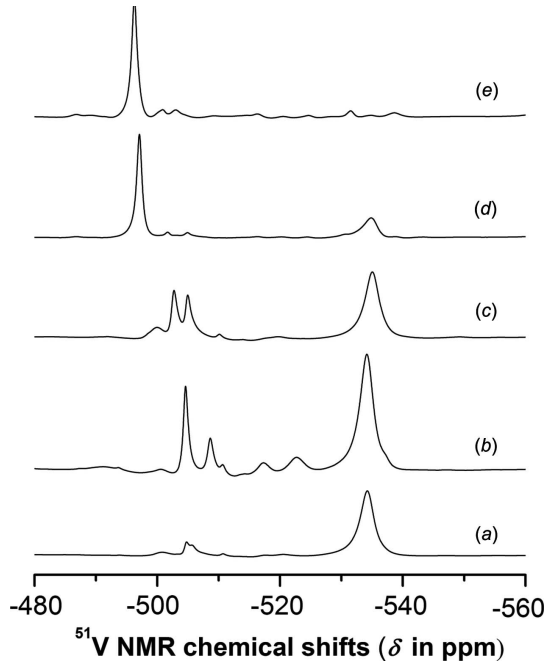

Figure 6
(*a*)/(*b*) The ^{51}V NMR spectra of the crystallization solution of **VMo$_7$** and (*c*)/(*d*)/(*e*) solutions obtained upon dissolution of crystallized **VMo$_7$** at different pH values. Conditions: (*a*) 175 m*M* Mo^{VI}, 25 m*M* V^V, pH = 3.1, 24 h after the synthesis; (*b*) same conditions as (*a*) after another 24 h; (*c*)/(*d*)/(*e*) 10 m*M* V^V solution prepared from **VMo$_7$** by dissolving it in 0.5 m*M* NaCl at pH values of (*c*) 4.0, (*d*) 5.2 and (*e*) 6.0. The pH was adjusted by the addition of a dilute KOH solution.

further details). All water molecules exhibit a certain degree of disorder and therefore we do not discuss the hydrogen-bond network. The water molecules complete an irregular coordination polyhedra around the potassium cations, forming a rich polymeric network based on electrostatic interactions (Fig. 4).

The IR spectrum of **VMo$_7$** (Fig. 5) exhibits bands typical for a *β*-octamolybdate structure and the respective bands corresponding to Mo—O or V—O vibrations are not distinguishable. The stretching vibrations of the terminal Mo/V═O units appear at 934 and 888 cm^{-1}, whereas the peaks in the region from 470 to 840 cm^{-1} correspond to the antisymmetric and symmetric deformation vibrations of the Mo—O—Mo and Mo—O—V bridging fragments. The crystallization water molecules exhibit typical bands for valence O—H vibrations and deformation H—O—H vibrations at 1610 and 3540 cm^{-1}, respectively.

We employed ^{51}V NMR spectroscopy to inspect the synthesis and hydrolytic stability of **VMo$_7$** (Fig. 6). All chemical shifts of the major species were assigned according to a very thorough speciation study based on NMR spectroscopy (^{51}V, ^{95}Mo and ^{17}O) and potentiometric data (Howarth *et al.*, 1991). In the crystallization solution one day after the synthesis (Fig. 4*a*), the $[VMo_7O_{26}]^{5-}$ anion (−534.2 ppm, 95% of V^V) is dominant, accompanied by a monovanadium-substituted hexamolybdate $[VMo_5O_{19}]^{3-}$ (−505.0 ppm) and some minor species. After two days (Fig. 4*b*), when about 33% of the product has crystallized out, roughly 73% of V^V is still

consumed in the $[VMo_7O_{26}]^{5-}$ species. Thus, the NMR investigation confirms that a synthetic protocol starting from reduced mixed Mo/V polyoxometalates oxidized by H_2O_2 leads almost exclusively to the desired $[VMo_7O_{26}]^{5-}$ anion. The speciation work by Howarth *et al.* proposed that $[VMo_7O_{26}]^{5-}$ should be most stable around pH = 4.2. At this pH value (Fig. 4*c*), we observed substantial decomposition of **VMo$_7$** into $[VMo_5O_{19}]^{3-}$ (−505.1 ppm) and α-$[VMo_7O_{26}]^{4-}$, a structure that resembles the Anderson–Evans archetype polyoxometalate capped by one Mo═O and one V═O unit (−502.9 ppm). Increased pH (Figs. 4*d* and 4*e*) results in a profound decomposition of $[VMo_7O_{26}]^{5-}$ into hexametalate $[V_2Mo_4O_{19}]^{4-}$ (−497.0 and −496.3 ppm). The results of the ^{51}V NMR measurements showed that once the $[VMo_7O_{26}]^{5-}$ anion is selectively formed from suitable precursors, it stays relatively intact in the solution for at least 24 h. On the other hand, by dissolution of **VMo$_7$** in aqueous solution, hydrolysis takes place and the newly formed species, mostly $[VMo_5O_{19}]^{3-}$, α-$[VMo_7O_{26}]^{4-}$ and $[V_2Mo_4O_{19}]^{4-}$, cannot give rise to the formation of $[VMo_7O_{26}]^{5-}$ even under conditions when the equilibrium of the POM species should be favoured (0.5 *M* NaCl, pH = 4.2).

Acknowledgements

The authors are grateful to ao.Univ.-Prof. Mag. Dr. Markus Galanski (Universität Wien, Austria) for NMR measurements and Dr Marek Bujdoš (Comenius University in Bratislava, Slovakia) for elemental analyses.

Funding information

Funding for this research was provided by: Austrian Science Fund (FWF, grant No. M2200 to LK; award No. P27534 to AR); University of Vienna (contract to AR).

References

Bijelic, A., Aureliano, M. & Rompel, A. (2018). *Chem. Commun.* **54**, 1153–1169.
Bijelic, A., Aureliano, M. & Rompel, A. (2019). *Angew. Chem. Int. Ed.* **58**, 2980–2999.
Bijelic, A. & Rompel, A. (2015). *Coord. Chem. Rev.* **299**, 22–38.
Bijelic, A. & Rompel, A. (2017). *Acc. Chem. Res.* **50**, 1441–1448.
Botar, B., Kögerler, P. & Hill, C. L. (2005). *Chem. Commun.* pp. 3138–3140.
Brandenburg, K. (2006). *DIAMOND*. Crystal Impact GbR, Bonn, Germany.
Bruker (2016). *SADABS* and *SAINT*. Bruker AXS Inc., Madison, Wisconsin, USA.
Bruker (2018). *APEX3*. Bruker AXS Inc., Madison, Wisconsin, USA.
Clemente-Juan, J. M., Coronado, E. & Gaita-Ariño, A. (2012). *Chem. Soc. Rev.* **41**, 7464–7478.
Dolomanov, O. V., Bourhis, L. J., Gildea, R. J., Howard, J. A. K. & Puschmann, H. (2009). *J. Appl. Cryst.* **42**, 339–341.
Fei, F., An, H. Y., Meng, C. G., Wang, L. & Wang, H. (2015). *RSC Adv.* **5**, 18796–18805.
Fu, L., Gao, H., Yan, M., Li, S., Li, X., Dai, Z. & Liu, S. (2015). *Small*, **11**, 2938–2945.
Gumerova, N. I. & Rompel, A. (2018). *Nat. Rev. Chem.* **2**, article No. 0112.
Howarth, O. W., Pettersson, L. & Andersson, I. (1991). *J. Chem. Soc. Dalton Trans.* pp. 1799–1812.
Hübschle, C. B., Sheldrick, G. M. & Dittrich, B. (2011). *J. Appl. Cryst.* **44**, 1281–1284.
Jahr, K. F., Fuchs, J. & Preuss, F. (1963). *Chem. Ber.* **96**, 556–569.
Krivosudský, L., Schwendt, P., Gyepes, R. & Filo, J. (2014). *Inorg. Chem. Commun.* **49**, 48–51.
Li, J. M., Xu, L., Jiang, N., Zhao, L. L. & Li, F. (2011). *Struct. Chem.* **22**, 1339–1345.
Molitor, C., Bijelic, A. & Rompel, A. (2017). *IUCrJ*, **4**, 734–740.
Müller, A., Todea, A. M., van Slageren, J., Dressel, M., Bögge, H., Schmidtmann, M., Luban, M., Engelhardt, L. & Rusu, M. (2005). *Angew. Chem. Int. Ed.* **44**, 3857–3861.
Nakamura, S. & Ozeki, T. (2001). *J. Chem. Soc. Dalton Trans.* pp. 472–480.
Nenner, A.-M. (1985). *Acta Cryst.* C**41**, 1703–1707.
Odyakov, V. F., Zhizhina, E. G., Rodikova, Y. A. & Gogin, L. L. (2015). *Eur. J. Inorg. Chem.* **2015**, 3618–3631.
Ozeki, T., Kihara, H. & Ikeda, S. (1988). *Anal. Chem.* **60**, 2055–2059.
Pope, M. (1983). In *Heteropoly and Isopoly Oxometalates*. Berlin: Springer.
Schwendt, P., Tatiersky, J., Krivosudský, L. & Šimuneková, M. (2016). *Coord. Chem. Rev.* **318**, 135–157.
Sheldrick, G. M. (2008). *Acta Cryst.* A**64**, 112–122.
Sheldrick, G. M. (2015). *Acta Cryst.* C**71**, 3–8.
Song, Y.-F. & Tsunashima, R. (2012). *Chem. Soc. Rev.* **41**, 7384–7402.
Spek, A. L. (2009). *Acta Cryst.* D**65**, 148–155.
Streb, C. (2012). *Dalton Trans.* **41**, 1651–1659.
Streb, C., Kastner, K. & Tucher, J. (2019). *Phys. Sci. Rev.* In the press. doi:10.1515/psr-2017-0177.
Tucher, J., Wu, Y., Nye, L. C., Ivanovic-Burmazovic, I., Khusniyarov, M. M. & Streb, C. (2012). *Dalton Trans.* **41**, 9938–9943.
Wang, S.-S. & Yang, G.-Y. (2015). *Chem. Rev.* **115**, 4893–4962.
Zhao, Y., Gao, Q., Tao, R., Li, F., Sun, Z. & Xu, L. (2018). *Inorg. Chem. Commun.* **89**, 94–98.

supporting information

Acta Cryst. (2019). C**75**, 872-876 [https://doi.org/10.1107/S205322961900620X]

Regioselective synthesis and characterization of monovanadium-substituted *β*-octamolybdate $[VMo_7O_{26}]^{5-}$

Lukáš Krivosudský, Alexander Roller and Annette Rompel

Computing details

Data collection: *APEX3* (Bruker, 2018); cell refinement: *SAINT* (Bruker, 2016); data reduction: *SAINT* (Bruker, 2016); program(s) used to solve structure: *SHELXS97* (Sheldrick, 2008); program(s) used to refine structure: *SHELXL2018* (Sheldrick, 2015); molecular graphics: OLEX2 (Dolomanov *et al.*, 2009) and *DIAMOND* (Brandenburg, 2006); software used to prepare material for publication: *PLATON* (Spek, 2009) and ShelXle (Hübschle, *et al.*, 2011) and OLEX2 (Dolomanov *et al.*, 2009).

Pentapotassium [hexaikosaoxido(heptamolybdenumvanadium)]ate hexahydrate

Crystal data

$K_5[VMo_7O_{26}]\cdot 6H_2O$
M_r = 1442.12
Monoclinic, *C*2/*c*
a = 12.9356 (10) Å
b = 16.1978 (10) Å
c = 13.8618 (9) Å
β = 90.962 (4)°
V = 2904.0 (3) Å^3
Z = 4
F(000) = 2720
D_x = 3.298 Mg m^{-3}
Mo *Kα* radiation, *λ* = 0.71073 Å
Cell parameters from 9243 reflections
θ = 3.5–30.0°
μ = 4.06 mm^{-1}
T = 143 K
Block, clear yellow
0.1 × 0.1 × 0.1 mm

Data collection

Bruker D8 Venture diffractometer
Radiation source: sealed xray tube, Incoatec IuS
φ and *ω* scans
Absorption correction: multi-scan (SADABS; Bruker, 2016)
T_{min} = 0.512, T_{max} = 0.564
80344 measured reflections
4259 independent reflections
4028 reflections with $I > 2\sigma(I)$
R_{int} = 0.057
θ_{max} = 30.1°, θ_{min} = 2.9°
h = −18→18
k = −22→22
l = −19→19

Refinement

Refinement on F^2
Least-squares matrix: full
$R[F^2 > 2\sigma(F^2)]$ = 0.027
$wR(F^2)$ = 0.059
S = 1.26
4259 reflections
235 parameters
37 restraints
Primary atom site location: heavy-atom method
H-atom parameters not defined
$w = 1/[\sigma^2(F_o^2) + (0.0001P)^2 + 32.0908P]$ where $P = (F_o^2 + 2F_c^2)/3$
$(\Delta/\sigma)_{max}$ = 0.002
$\Delta\rho_{max}$ = 0.64 e Å^{-3}
$\Delta\rho_{min}$ = −0.73 e Å^{-3}

Special details

Geometry. All esds (except the esd in the dihedral angle between two l.s. planes) are estimated using the full covariance matrix. The cell esds are taken into account individually in the estimation of esds in distances, angles and torsion angles; correlations between esds in cell parameters are only used when they are defined by crystal symmetry. An approximate (isotropic) treatment of cell esds is used for estimating esds involving l.s. planes.

Refinement. _olex2_refinement_description 1. Restrained distances K3-O17S ~ K4-O16S with sigma of 0.04 2. Uiso/Uaniso restraints and constraints Uanis(O16S) ~ Ueq, Uanis(O17S) ~ Ueq: with sigma of 0.02 and sigma for terminal atoms of 0.04 Uanis(K4) ~ Ueq, Uanis(K3) ~ Ueq: with sigma of 0.05 and sigma for terminal atoms of 0.1 Uanis(O19S) ~ Ueq, Uanis(O18S) ~ Ueq: with sigma of 0.02 and sigma for terminal atoms of 0.04 Uanis(Mo4A) = Uanis(V4) 3. Others Fixed Sof: V4(0.5) K3(0.6) O17S(0.3) Mo4A(0.5) K4(0.4) O16S(0.2) O19S(0.3) O18S(0.2)

Fractional atomic coordinates and isotropic or equivalent isotropic displacement parameters (Å²)

	x	*y*	*z*	U_{iso}*/U_{eq}	Occ. (<1)
Mo1	0.60579 (2)	0.38037 (2)	0.98066 (2)	0.01081 (6)	
Mo2	0.47932 (2)	0.21300 (2)	1.03581 (2)	0.01181 (6)	
Mo3	0.65441 (2)	0.10564 (2)	0.92676 (2)	0.01002 (6)	
K1	0.500000	0.25427 (7)	0.750000	0.01348 (19)	
K2	0.31406 (6)	0.37807 (5)	0.90717 (7)	0.02218 (17)	
O1	0.54136 (19)	0.38311 (16)	0.87068 (19)	0.0154 (5)	
O2	0.41768 (19)	0.22432 (16)	0.92545 (19)	0.0162 (5)	
O3	0.59213 (19)	0.11548 (16)	0.81722 (18)	0.0151 (5)	
O4	0.7111 (2)	0.27748 (16)	0.7712 (2)	0.0172 (5)	
O5	0.60418 (19)	0.47897 (16)	1.0214 (2)	0.0172 (5)	
O6	0.3830 (2)	0.19028 (17)	1.1137 (2)	0.0181 (5)	
O7	0.68024 (19)	0.00256 (16)	0.9364 (2)	0.0157 (5)	
O8	0.90217 (19)	0.28854 (16)	0.84839 (18)	0.0134 (5)	
O9	0.74853 (18)	0.37746 (15)	0.93218 (17)	0.0116 (4)	
O10	0.50256 (18)	0.32975 (15)	1.05790 (18)	0.0132 (5)	
O11	0.54021 (18)	0.10735 (15)	1.01354 (18)	0.0129 (5)	
O12	0.78897 (18)	0.15146 (15)	0.89034 (18)	0.0121 (4)	
O13	0.64659 (18)	0.24183 (15)	0.96599 (18)	0.0129 (5)	
O14S	0.3275 (3)	0.4852 (2)	0.7528 (3)	0.0392 (8)	
O15S	0.7757 (3)	−0.1362 (2)	1.1084 (3)	0.0349 (8)	
V4	0.7746 (9)	0.2690 (7)	0.8831 (6)	0.0071 (3)	0.5
K3	0.6350 (7)	−0.0145 (4)	1.1512 (5)	0.0478 (15)	0.6
O17S	0.4632 (12)	0.0633 (9)	1.2324 (15)	0.020 (3)	0.3
Mo4A	0.7748 (4)	0.2706 (4)	0.8710 (2)	0.0071 (3)	0.5
K4	0.6247 (10)	−0.0282 (6)	1.1377 (7)	0.0296 (16)	0.4
O16S	0.500000	0.0715 (14)	1.250000	0.029 (6)	0.4
O19S	0.533 (2)	0.3893 (13)	1.262 (2)	0.033 (6)	0.3
O18S	0.500000	0.3867 (16)	1.250000	0.025 (7)	0.4

Atomic displacement parameters (Å²)

	U^{11}	U^{22}	U^{33}	U^{12}	U^{13}	U^{23}
Mo1	0.00751 (12)	0.01082 (13)	0.01402 (13)	0.00096 (9)	−0.00248 (10)	−0.00156 (10)
Mo2	0.00759 (12)	0.01365 (13)	0.01420 (13)	−0.00028 (10)	0.00014 (10)	−0.00243 (10)

Mo3	0.00816 (12)	0.01032 (13)	0.01151 (13)	0.00031 (9)	−0.00168 (9)	−0.00177 (10)
K1	0.0131 (4)	0.0150 (5)	0.0122 (4)	0.000	−0.0029 (3)	0.000
K2	0.0140 (3)	0.0156 (4)	0.0369 (5)	0.0019 (3)	−0.0020 (3)	−0.0053 (3)
O1	0.0117 (11)	0.0172 (12)	0.0170 (12)	0.0011 (9)	−0.0047 (9)	−0.0013 (10)
O2	0.0116 (11)	0.0172 (12)	0.0196 (13)	0.0007 (9)	−0.0029 (9)	−0.0024 (10)
O3	0.0133 (11)	0.0164 (12)	0.0154 (12)	−0.0002 (9)	−0.0037 (9)	−0.0028 (10)
O4	0.0132 (11)	0.0174 (12)	0.0210 (13)	−0.0010 (9)	−0.0002 (10)	0.0028 (10)
O5	0.0117 (11)	0.0155 (12)	0.0242 (13)	0.0012 (9)	−0.0044 (10)	−0.0042 (10)
O6	0.0124 (11)	0.0197 (13)	0.0222 (13)	−0.0030 (10)	0.0034 (10)	−0.0039 (10)
O7	0.0115 (11)	0.0133 (12)	0.0222 (13)	0.0004 (9)	−0.0015 (10)	−0.0013 (10)
O8	0.0117 (11)	0.0160 (12)	0.0124 (11)	−0.0007 (9)	−0.0010 (9)	0.0001 (9)
O9	0.0093 (10)	0.0113 (11)	0.0140 (11)	0.0000 (8)	−0.0019 (9)	0.0013 (9)
O10	0.0101 (11)	0.0132 (11)	0.0163 (12)	0.0011 (9)	0.0010 (9)	−0.0050 (9)
O11	0.0104 (11)	0.0135 (11)	0.0149 (11)	−0.0008 (9)	0.0013 (9)	−0.0001 (9)
O12	0.0097 (10)	0.0122 (11)	0.0143 (11)	0.0000 (8)	−0.0016 (9)	−0.0006 (9)
O13	0.0098 (11)	0.0120 (11)	0.0167 (12)	0.0002 (9)	−0.0011 (9)	−0.0001 (9)
O14S	0.052 (2)	0.039 (2)	0.0263 (17)	0.0065 (17)	−0.0009 (16)	−0.0059 (15)
O15S	0.0313 (17)	0.0275 (17)	0.046 (2)	−0.0023 (14)	−0.0003 (15)	0.0006 (15)
V4	0.00768 (16)	0.0105 (3)	0.0031 (9)	−0.00021 (16)	−0.0007 (7)	0.0010 (7)
K3	0.0307 (14)	0.063 (4)	0.050 (3)	0.015 (2)	0.014 (2)	0.038 (2)
O17S	0.031 (9)	0.010 (5)	0.019 (6)	−0.003 (6)	0.001 (6)	−0.002 (4)
Mo4A	0.00768 (16)	0.0105 (3)	0.0031 (9)	−0.00021 (16)	−0.0007 (7)	0.0010 (7)
K4	0.047 (4)	0.0252 (17)	0.0172 (15)	0.0130 (19)	0.0138 (18)	0.0008 (12)
O16S	0.037 (13)	0.021 (8)	0.029 (13)	0.000	0.018 (11)	0.000
O19S	0.049 (17)	0.041 (8)	0.008 (8)	−0.027 (9)	0.001 (10)	−0.008 (5)
O18S	0.036 (19)	0.017 (8)	0.021 (13)	0.000	−0.014 (12)	0.000

Geometric parameters (Å, º)

Mo1—K1	4.0151 (6)	K2—O1	2.993 (3)
Mo1—K2	3.8924 (9)	K2—O2	2.838 (3)
Mo1—O1	1.726 (3)	K2—O4^{iii}	2.975 (3)
Mo1—O5	1.694 (3)	K2—O5^{iv}	2.725 (3)
Mo1—O9	1.976 (2)	K2—O6^{v}	2.790 (3)
Mo1—O10	1.910 (3)	K2—O7^{vi}	2.693 (3)
Mo1—O12^{i}	2.288 (2)	K2—O10	3.279 (3)
Mo1—O13	2.315 (2)	K2—O14S	2.763 (4)
Mo1—V4	3.155 (12)	K2—O15S^{vi}	2.850 (4)
Mo1—Mo4A	3.219 (5)	O2—K4^{ii}	3.339 (9)
Mo2—K1	4.0312 (4)	O3—K3^{ii}	3.398 (9)
Mo2—K2	3.8433 (9)	O3—K3^{vii}	2.884 (9)
Mo2—O2	1.723 (3)	O3—K4^{ii}	3.212 (13)
Mo2—O6	1.702 (3)	O3—K4^{vii}	2.899 (12)
Mo2—O8^{i}	2.201 (2)	O4—V4	1.748 (9)
Mo2—O10	1.938 (2)	O4—Mo4A	1.601 (5)
Mo2—O11	1.911 (3)	O7—K3	3.056 (8)
Mo2—O13	2.430 (2)	O7—K4	2.935 (11)
Mo2—K4^{ii}	4.056 (8)	O8—V4	1.755 (12)

Mo3—K1	3.9529 (7)	O8—Mo4A	1.708 (6)
Mo3—O3	1.714 (3)	O9—V4	1.916 (12)
Mo3—O7	1.708 (3)	O9—K3^{i}	2.931 (9)
Mo3—O9^{i}	2.322 (2)	O9—Mo4A	1.960 (6)
Mo3—O11	1.921 (2)	O9—K4^{i}	3.105 (13)
Mo3—O12	1.966 (2)	O11—K3	2.994 (8)
Mo3—O13	2.275 (2)	O11—K4^{ii}	3.232 (11)
Mo3—V4	3.134 (12)	O11—K4	2.986 (12)
Mo3—K3	3.682 (8)	O12—V4	1.916 (12)
Mo3—Mo4A	3.194 (6)	O12—Mo4A	1.956 (6)
Mo3—K4	3.665 (12)	O13—V4^{i}	2.318 (9)
Mo3—K4^{ii}	3.912 (13)	O13—V4	2.079 (11)
K1—K2^{iii}	3.8378 (10)	O13—Mo4A	2.185 (6)
K1—K2	3.8378 (10)	O13—Mo4A^{i}	2.471 (5)
K1—O1^{iii}	2.722 (3)	O14S—K3^{viii}	2.879 (9)
K1—O1	2.722 (3)	O14S—K4^{viii}	3.125 (13)
K1—O2	2.715 (3)	O15S—K3	2.753 (8)
K1—O2^{iii}	2.715 (3)	O15S—K4	2.658 (11)
K1—O3^{iii}	2.703 (3)	K3—K3^{ix}	4.475 (16)
K1—O3	2.703 (3)	K3—O17S	2.808 (17)
K1—O4	2.767 (3)	K3—O17S^{ix}	2.42 (2)
K1—O4^{iii}	2.767 (3)	O17S—O17S^{ix}	1.06 (3)
K1—Mo4A^{iii}	3.913 (5)	K4—O16S	2.778 (15)
K1—Mo4A	3.913 (5)	O19S—O19S^{ix}	0.91 (5)

K2—Mo1—K1	58.044 (15)	Mo2—O2—K4^{ii}	101.7 (2)
O1—Mo1—K1	32.49 (9)	K1—O2—K2	87.42 (8)
O1—Mo1—K2	46.95 (9)	K1—O2—K4^{ii}	90.0 (2)
O1—Mo1—O9	98.07 (11)	K2—O2—K4^{ii}	137.4 (2)
O1—Mo1—O10	100.05 (12)	Mo3—O3—K1	125.49 (13)
O1—Mo1—O12^{i}	165.57 (11)	Mo3—O3—K3^{ii}	103.63 (17)
O1—Mo1—O13	93.14 (11)	Mo3—O3—K3^{vii}	124.1 (2)
O1—Mo1—V4	87.91 (19)	Mo3—O3—K4^{ii}	100.7 (2)
O1—Mo1—Mo4A	85.33 (11)	Mo3—O3—K4^{vii}	129.9 (3)
O5—Mo1—K1	137.65 (9)	K1—O3—K3^{vii}	106.62 (16)
O5—Mo1—K2	94.53 (9)	K1—O3—K3^{ii}	93.86 (15)
O5—Mo1—O1	105.17 (13)	K1—O3—K4^{vii}	100.3 (2)
O5—Mo1—O9	98.78 (11)	K1—O3—K4^{ii}	93.0 (2)
O5—Mo1—O10	101.84 (12)	K3^{vii}—O3—K3^{ii}	90.5 (2)
O5—Mo1—O12^{i}	87.84 (11)	K3^{vii}—O3—K4^{vii}	6.3 (3)
O5—Mo1—O13	161.28 (11)	K3^{vii}—O3—K4^{ii}	94.93 (18)
O5—Mo1—V4	134.0 (2)	K1—O4—K2^{iii}	83.81 (7)
O5—Mo1—Mo4A	133.66 (14)	V4—O4—K1	122.2 (4)
O9—Mo1—K1	91.43 (7)	V4—O4—K2^{iii}	145.4 (4)
O9—Mo1—K2	144.89 (7)	Mo4A—O4—K1	125.1 (2)
O9—Mo1—O12^{i}	73.34 (9)	Mo1—O5—K2^{iv}	156.25 (14)
O9—Mo1—O13	74.41 (9)	Mo2—O6—K2^{v}	134.22 (14)
O9—Mo1—V4	35.2 (2)	Mo3—O7—K2^{x}	147.76 (14)

O9—Mo1—Mo4A	34.96 (12)	Mo3—O7—K3	97.17 (17)
O10—Mo1—K1	89.77 (7)	Mo3—O7—K4	100.9 (2)
O10—Mo1—K2	57.24 (8)	K2^{x}—O7—K3	102.29 (16)
O10—Mo1—O9	147.81 (10)	K2^{x}—O7—K4	100.6 (2)
O10—Mo1—O12^{i}	82.97 (10)	V4—O8—Mo2^{i}	116.4 (3)
O10—Mo1—O13	78.22 (10)	Mo1—O9—Mo3^{i}	101.88 (10)
O10—Mo1—V4	119.4 (2)	Mo1—O9—K3^{i}	127.24 (18)
O10—Mo1—Mo4A	120.94 (12)	Mo1—O9—K4^{i}	126.1 (2)
O12^{i}—Mo1—K1	134.28 (6)	Mo3^{i}—O9—K3^{i}	88.20 (17)
O12^{i}—Mo1—K2	139.81 (6)	Mo3^{i}—O9—K4^{i}	83.6 (2)
O12^{i}—Mo1—O13	73.54 (9)	V4—O9—Mo1	108.3 (4)
O12^{i}—Mo1—V4	78.41 (17)	V4—O9—Mo3^{i}	108.1 (3)
O12^{i}—Mo1—Mo4A	81.08 (10)	V4—O9—K3^{i}	117.4 (3)
O13—Mo1—K1	60.80 (6)	V4—O9—K4^{i}	120.9 (4)
O13—Mo1—K2	100.91 (6)	K3^{i}—O9—K4^{i}	5.0 (3)
O13—Mo1—V4	41.2 (2)	Mo4A—O9—Mo1	109.7 (2)
O13—Mo1—Mo4A	42.73 (11)	Mo1—O10—Mo2	115.99 (12)
V4—Mo1—K1	66.23 (19)	Mo1—O10—K2	93.43 (9)
V4—Mo1—K2	123.9 (2)	Mo2—O10—K2	91.18 (9)
Mo4A—Mo1—K1	64.40 (9)	Mo2—O11—Mo3	115.94 (13)
Mo4A—Mo1—K2	122.28 (9)	Mo2—O11—K3	130.77 (16)
K1—Mo2—K4^{ii}	64.30 (17)	Mo2—O11—K4^{ii}	101.0 (2)
K2—Mo2—K1	58.277 (18)	Mo2—O11—K4	135.48 (18)
K2—Mo2—K4^{ii}	93.55 (18)	Mo3—O11—K3	94.50 (18)
O2—Mo2—K1	31.47 (9)	Mo3—O11—K4	94.2 (2)
O2—Mo2—K2	42.99 (9)	Mo3—O11—K4^{ii}	95.4 (2)
O2—Mo2—O8^{i}	162.74 (11)	K3—O11—K4^{ii}	114.3 (3)
O2—Mo2—O10	96.00 (12)	Mo3—O12—Mo1^{i}	103.41 (11)
O2—Mo2—O11	97.91 (12)	V4—O12—Mo1^{i}	108.7 (3)
O2—Mo2—O13	91.59 (11)	V4—O12—Mo3	107.7 (4)
O2—Mo2—K4^{ii}	53.7 (2)	Mo4A—O12—Mo3	109.0 (2)
O6—Mo2—K1	136.08 (9)	Mo1—O13—Mo2	86.88 (8)
O6—Mo2—K2	92.13 (10)	Mo1—O13—V4^{i}	95.3 (3)
O6—Mo2—O2	104.67 (13)	Mo1—O13—Mo4A^{i}	95.14 (16)
O6—Mo2—O8^{i}	92.49 (11)	Mo2—O13—Mo4A^{i}	88.62 (15)
O6—Mo2—O10	102.94 (12)	Mo3—O13—Mo1	166.46 (12)
O6—Mo2—O11	102.53 (12)	Mo3—O13—Mo2	87.26 (8)
O6—Mo2—O13	163.74 (11)	Mo3—O13—V4^{i}	97.0 (3)
O6—Mo2—K4^{ii}	88.7 (2)	Mo3—O13—Mo4A^{i}	96.92 (16)
O8^{i}—Mo2—K1	131.43 (7)	V4—O13—Mo1	91.6 (3)
O8^{i}—Mo2—K2	136.17 (7)	V4^{i}—O13—Mo2	90.4 (3)
O8^{i}—Mo2—O13	71.26 (9)	V4—O13—Mo2	169.7 (3)
O8^{i}—Mo2—K4^{ii}	130.11 (19)	V4—O13—Mo3	92.0 (3)
O10—Mo2—K1	88.90 (8)	V4—O13—V4^{i}	99.9 (3)
O10—Mo2—K2	58.54 (7)	V4—O13—Mo4A^{i}	101.7 (4)
O10—Mo2—O8^{i}	77.97 (10)	V4^{i}—O13—Mo4A^{i}	1.8 (4)
O10—Mo2—O13	74.85 (9)	Mo4A—O13—Mo1	91.30 (18)
O10—Mo2—K4^{ii}	149.63 (19)	Mo4A—O13—Mo2	166.09 (17)

O11—Mo2—K1	87.44 (8)	Mo4A—O13—Mo3	91.45 (18)
O11—Mo2—K2	140.85 (8)	K2—O14S—K3^{viii}	114.69 (19)
O11—Mo2—O8^{i}	79.85 (10)	K2—O14S—K4^{viii}	118.2 (2)
O11—Mo2—O10	146.71 (10)	K3^{viii}—O14S—K4^{viii}	3.8 (3)
O11—Mo2—O13	74.67 (9)	K3—O15S—K2^{x}	106.2 (2)
O11—Mo2—K4^{ii}	51.45 (19)	Mo1—V4—K1	67.3 (2)
O13—Mo2—K1	60.17 (6)	Mo3—V4—Mo1	92.9 (3)
O13—Mo2—K2	99.99 (6)	Mo3—V4—K1	66.2 (2)
O13—Mo2—K4^{ii}	101.21 (18)	O4—V4—Mo1	91.0 (5)
O3—Mo3—K1	33.83 (9)	O4—V4—Mo3	90.6 (5)
O3—Mo3—O9^{i}	166.97 (11)	O4—V4—K1	36.0 (3)
O3—Mo3—O11	101.45 (11)	O4—V4—O8	100.0 (5)
O3—Mo3—O12	98.18 (11)	O4—V4—O9	99.2 (6)
O3—Mo3—O13	95.71 (11)	O4—V4—O12	99.7 (5)
O3—Mo3—V4	88.72 (19)	O4—V4—O13^{i}	178.0 (7)
O3—Mo3—K3	139.46 (16)	O4—V4—O13	98.0 (6)
O3—Mo3—Mo4A	86.07 (12)	O8—V4—Mo1	132.5 (6)
O3—Mo3—K4^{ii}	53.79 (19)	O8—V4—Mo3	132.6 (6)
O3—Mo3—K4	135.1 (2)	O8—V4—K1	136.0 (4)
O7—Mo3—K1	137.77 (9)	O8—V4—O9	96.0 (6)
O7—Mo3—O3	104.41 (13)	O8—V4—O12	95.9 (6)
O7—Mo3—O9^{i}	86.95 (11)	O8—V4—O13	162.0 (5)
O7—Mo3—O11	96.69 (12)	O8—V4—O13^{i}	82.0 (4)
O7—Mo3—O12	102.49 (11)	O9—V4—Mo1	36.5 (2)
O7—Mo3—O13	159.87 (11)	O9—V4—Mo3	127.9 (5)
O7—Mo3—V4	138.1 (2)	O9—V4—K1	93.3 (4)
O7—Mo3—K3	55.44 (13)	O9—V4—O13	81.4 (4)
O7—Mo3—Mo4A	137.85 (14)	O9—V4—O13^{i}	80.0 (4)
O7—Mo3—K4^{ii}	83.28 (18)	O12—V4—Mo1	127.8 (5)
O7—Mo3—K4	51.84 (15)	O12—V4—Mo3	36.7 (2)
O9^{i}—Mo3—K1	135.28 (6)	O12—V4—K1	92.8 (4)
O9^{i}—Mo3—V4	78.46 (17)	O12—V4—O9	155.5 (5)
O9^{i}—Mo3—K3	52.73 (14)	O12—V4—O13^{i}	80.6 (4)
O9^{i}—Mo3—Mo4A	81.16 (9)	O12—V4—O13	80.7 (4)
O9^{i}—Mo3—K4	57.34 (18)	O13^{i}—V4—Mo1	87.3 (3)
O9^{i}—Mo3—K4^{ii}	135.58 (17)	O13—V4—Mo1	47.2 (2)
O11—Mo3—K1	89.63 (7)	O13—V4—Mo3	46.5 (2)
O11—Mo3—O9^{i}	83.21 (9)	O13^{i}—V4—Mo3	88.5 (3)
O11—Mo3—O12	148.10 (10)	O13^{i}—V4—K1	142.1 (4)
O11—Mo3—O13	78.38 (10)	O13—V4—K1	62.0 (3)
O11—Mo3—V4	119.9 (2)	O13—V4—O13^{i}	80.1 (3)
O11—Mo3—K3	54.17 (14)	Mo3—K3—Mo3^{xi}	166.9 (2)
O11—Mo3—Mo4A	121.51 (12)	Mo3^{xi}—K3—K3^{ix}	57.71 (14)
O11—Mo3—K4	54.33 (19)	Mo3—K3—K3^{ix}	125.6 (3)
O11—Mo3—K4^{ii}	55.33 (15)	O3^{xi}—K3—Mo3^{xi}	20.28 (8)
O12—Mo3—K1	92.94 (7)	O3^{ii}—K3—Mo3^{xi}	75.30 (16)
O12—Mo3—O9^{i}	72.73 (9)	O3^{xi}—K3—Mo3	172.1 (3)
O12—Mo3—O13	74.84 (9)	O3^{ii}—K3—Mo3	115.8 (2)

O12—Mo3—V4	35.6 (2)	O3^{xi}—K3—O3^{ii}	56.36 (18)
O12—Mo3—K3	119.32 (15)	O3^{xi}—K3—O7	150.6 (2)
O12—Mo3—Mo4A	35.39 (13)	O3^{xi}—K3—O9^{i}	148.3 (3)
O12—Mo3—K4^{ii}	151.67 (18)	O3^{xi}—K3—O11	143.1 (3)
O12—Mo3—K4	122.2 (2)	O3^{xi}—K3—K3^{ix}	49.39 (13)
O13—Mo3—K1	62.19 (6)	O3^{ii}—K3—K3^{ix}	40.13 (14)
O13—Mo3—O9^{i}	73.14 (9)	O7—K3—Mo3^{xi}	158.6 (2)
O13—Mo3—V4	41.5 (2)	O7—K3—Mo3	27.39 (9)
O13—Mo3—K3	107.87 (11)	O7—K3—O3^{ii}	110.4 (2)
O13—Mo3—Mo4A	43.15 (11)	O7—K3—K3^{ix}	139.5 (3)
O13—Mo3—K4^{ii}	108.73 (15)	O9^{i}—K3—Mo3	39.07 (11)
O13—Mo3—K4	112.15 (12)	O9^{i}—K3—Mo3^{xi}	128.1 (2)
V4—Mo3—K1	67.24 (19)	O9^{i}—K3—O3^{ii}	150.1 (3)
V4—Mo3—K3	130.6 (2)	O9^{i}—K3—O7	55.89 (16)
V4—Mo3—K4^{ii}	133.3 (3)	O9^{i}—K3—O11	57.11 (17)
K3—Mo3—K1	143.60 (13)	O9^{i}—K3—K3^{ix}	130.75 (13)
K3—Mo3—K4^{ii}	87.0 (2)	O11—K3—Mo3^{xi}	148.1 (2)
Mo4A—Mo3—K1	65.40 (9)	O11—K3—Mo3	31.33 (9)
Mo4A—Mo3—K4	138.23 (18)	O11—K3—O3^{ii}	93.1 (2)
K4^{ii}—Mo3—K1	66.35 (18)	O11—K3—O7	53.30 (15)
K4—Mo3—K1	142.8 (2)	O11—K3—K3^{ix}	94.3 (2)
K2—K1—K2^{iii}	117.00 (4)	O14S^{xii}—K3—Mo3	104.8 (3)
K2^{iii}—K1—Mo4A^{iii}	107.15 (7)	O14S^{xii}—K3—Mo3^{xi}	64.19 (16)
K2^{iii}—K1—Mo4A	68.57 (6)	O14S^{xii}—K3—O3^{ii}	139.4 (3)
K2—K1—Mo4A^{iii}	68.57 (6)	O14S^{xii}—K3—O3^{xi}	83.1 (2)
K2—K1—Mo4A	107.15 (8)	O14S^{xii}—K3—O7	106.5 (3)
O1^{iii}—K1—K2	80.20 (6)	O14S^{xii}—K3—O9^{i}	67.8 (2)
O1—K1—K2^{iii}	80.20 (6)	O14S^{xii}—K3—O11	123.0 (3)
O1—K1—K2	50.89 (6)	O14S^{xii}—K3—K3^{ix}	112.2 (3)
O1^{iii}—K1—K2^{iii}	50.89 (6)	O15S—K3—Mo3	98.1 (2)
O1—K1—O1^{iii}	79.89 (11)	O15S—K3—Mo3^{xi}	85.0 (2)
O1—K1—O4	69.33 (8)	O15S—K3—O3^{ii}	105.0 (2)
O1—K1—O4^{iii}	98.31 (8)	O15S—K3—O3^{xi}	84.4 (2)
O1^{iii}—K1—O4	98.31 (8)	O15S—K3—O7	73.55 (18)
O1^{iii}—K1—O4^{iii}	69.33 (8)	O15S—K3—O9^{i}	96.4 (3)
O1^{iii}—K1—Mo4A^{iii}	61.13 (10)	O15S—K3—O11	126.8 (3)
O1—K1—Mo4A^{iii}	112.29 (9)	O15S—K3—O14S^{xii}	69.8 (2)
O1^{iii}—K1—Mo4A	112.29 (9)	O15S—K3—K3^{ix}	131.1 (2)
O1—K1—Mo4A	61.13 (10)	O15S—K3—O17S	159.8 (5)
O2—K1—K2	47.61 (6)	O17S^{ix}—K3—Mo3^{xi}	65.9 (4)
O2^{iii}—K1—K2	149.41 (6)	O17S^{ix}—K3—Mo3	109.3 (4)
O2^{iii}—K1—K2^{iii}	47.61 (6)	O17S—K3—Mo3^{xi}	79.9 (5)
O2—K1—K2^{iii}	149.41 (6)	O17S—K3—Mo3	99.6 (5)
O2—K1—O1	70.28 (8)	O17S^{ix}—K3—O3^{ii}	72.6 (5)
O2—K1—O1^{iii}	127.70 (8)	O17S^{ix}—K3—O3^{xi}	69.8 (4)
O2^{iii}—K1—O1	127.70 (8)	O17S—K3—O3^{xi}	76.7 (5)
O2^{iii}—K1—O1^{iii}	70.27 (8)	O17S—K3—O3^{ii}	58.1 (3)
O2—K1—O2^{iii}	159.41 (12)	O17S^{ix}—K3—O7	135.4 (5)

O2—K1—O4^{iii}	73.65 (8)	O17S—K3—O7	121.0 (5)
O2—K1—O4	109.28 (8)	O17S^{ix}—K3—O9^{i}	98.4 (4)
O2^{iii}—K1—O4^{iii}	109.28 (8)	O17S—K3—O9^{i}	103.5 (4)
O2^{iii}—K1—O4	73.65 (8)	O17S—K3—O11	68.9 (5)
O2—K1—Mo4A^{iii}	91.66 (8)	O17S^{ix}—K3—O11	82.4 (4)
O2^{iii}—K1—Mo4A	91.66 (8)	O17S—K3—O14S^{xii}	114.4 (4)
O2^{iii}—K1—Mo4A^{iii}	89.73 (8)	O17S^{ix}—K3—O14S^{xii}	92.7 (5)
O2—K1—Mo4A	89.73 (8)	O17S^{ix}—K3—O15S	150.6 (5)
O3—K1—K2^{iii}	110.69 (6)	O17S^{ix}—K3—K3^{ix}	33.9 (4)
O3^{iii}—K1—K2	110.69 (6)	O17S—K3—K3^{ix}	28.7 (4)
O3^{iii}—K1—K2^{iii}	121.05 (6)	O17S^{ix}—K3—O17S	21.9 (7)
O3—K1—K2	121.05 (6)	K3^{ix}—O17S—K3	117.4 (8)
O3—K1—O1	110.17 (7)	O17S^{ix}—O17S—K3	58.3 (17)
O3^{iii}—K1—O1^{iii}	110.17 (7)	O17S^{ix}—O17S—K3^{ix}	100 (2)
O3—K1—O1^{iii}	158.51 (8)	Mo1—Mo4A—K1	67.71 (10)
O3^{iii}—K1—O1	158.51 (8)	Mo3—Mo4A—Mo1	90.58 (13)
O3^{iii}—K1—O2^{iii}	73.73 (8)	Mo3—Mo4A—K1	66.70 (10)
O3—K1—O2	73.73 (8)	O4—Mo4A—Mo1	91.5 (2)
O3^{iii}—K1—O2	89.02 (8)	O4—Mo4A—Mo3	91.2 (2)
O3—K1—O2^{iii}	89.02 (8)	O4—Mo4A—K1	35.35 (17)
O3—K1—O3^{iii}	67.44 (11)	O4—Mo4A—O8	108.3 (3)
O3—K1—O4	69.37 (8)	O4—Mo4A—O9	102.8 (3)
O3—K1—O4^{iii}	125.33 (8)	O4—Mo4A—O12	103.5 (3)
O3^{iii}—K1—O4	125.33 (8)	O4—Mo4A—O13	98.7 (3)
O3^{iii}—K1—O4^{iii}	69.37 (8)	O4—Mo4A—O13^{i}	173.3 (3)
O3—K1—Mo4A^{iii}	126.58 (10)	O8—Mo4A—Mo1	131.1 (3)
O3^{iii}—K1—Mo4A^{iii}	61.08 (10)	O8—Mo4A—Mo3	131.5 (3)
O3^{iii}—K1—Mo4A	126.58 (10)	O8—Mo4A—K1	143.64 (18)
O3—K1—Mo4A	61.08 (10)	O8—Mo4A—O9	95.9 (3)
O4—K1—K2^{iii}	50.41 (6)	O8—Mo4A—O12	96.0 (3)
O4^{iii}—K1—K2	50.41 (6)	O8—Mo4A—O13	153.0 (2)
O4^{iii}—K1—K2^{iii}	119.69 (6)	O8—Mo4A—O13^{i}	78.3 (2)
O4—K1—K2	119.69 (6)	O9—Mo4A—Mo1	35.29 (12)
O4^{iii}—K1—O4	164.38 (12)	O9—Mo4A—Mo3	123.1 (2)
O4—K1—Mo4A	19.56 (8)	O9—Mo4A—K1	94.7 (2)
O4^{iii}—K1—Mo4A^{iii}	19.56 (8)	O9—Mo4A—O13	77.8 (2)
O4^{iii}—K1—Mo4A	157.51 (9)	O9—Mo4A—O13^{i}	75.38 (16)
O4—K1—Mo4A^{iii}	157.51 (9)	O12—Mo4A—Mo1	122.9 (2)
Mo4A^{iii}—K1—Mo4A	172.26 (17)	O12—Mo4A—Mo3	35.59 (12)
Mo2—K2—Mo1	49.905 (12)	O12—Mo4A—K1	94.3 (2)
K1—K2—Mo1	62.579 (15)	O12—Mo4A—O9	145.9 (2)
K1—K2—Mo2	63.312 (16)	O12—Mo4A—O13	77.1 (2)
O1—K2—Mo1	24.92 (5)	O12—Mo4A—O13^{i}	75.99 (17)
O1—K2—Mo2	63.71 (5)	O13^{i}—Mo4A—Mo1	83.42 (13)
O1—K2—K1	44.89 (5)	O13—Mo4A—Mo1	45.97 (12)
O1—K2—O10	52.56 (7)	O13^{i}—Mo4A—Mo3	84.57 (14)
O2—K2—Mo1	62.00 (5)	O13—Mo4A—Mo3	45.40 (12)
O2—K2—Mo2	24.46 (5)	O13^{i}—Mo4A—K1	138.03 (18)

O2—K2—K1	44.97 (6)	O13—Mo4A—K1	63.32 (14)
O2—K2—O1	64.86 (8)	O13—Mo4A—O13^{i}	74.71 (14)
O2—K2—O4^{iii}	68.80 (8)	Mo3—K4—Mo3^{ii}	96.7 (3)
O2—K2—O10	52.30 (7)	O2^{ii}—K4—Mo3^{ii}	59.19 (19)
O2—K2—O15S^{vi}	86.06 (9)	O2^{ii}—K4—Mo3	111.9 (2)
O4^{iii}—K2—Mo1	108.35 (5)	O3^{ii}—K4—Mo3^{ii}	25.51 (11)
O4^{iii}—K2—Mo2	93.26 (6)	O3^{ii}—K4—Mo3	121.3 (4)
O4^{iii}—K2—K1	45.79 (5)	O3^{xi}—K4—Mo3	172.7 (3)
O4^{iii}—K2—O1	88.19 (7)	O3^{xi}—K4—Mo3^{ii}	83.8 (3)
O4^{iii}—K2—O10	117.95 (7)	O3^{ii}—K4—O2^{ii}	59.5 (2)
O5^{iv}—K2—Mo1	61.84 (6)	O3^{xi}—K4—O2^{ii}	74.6 (3)
O5^{iv}—K2—Mo2	102.31 (6)	O3^{xi}—K4—O3^{ii}	58.5 (3)
O5^{iv}—K2—K1	114.02 (6)	O3^{xi}—K4—O7	160.0 (3)
O5^{iv}—K2—O1	70.23 (8)	O3^{xi}—K4—O9^{i}	137.5 (4)
O5^{iv}—K2—O2	122.24 (8)	O3^{ii}—K4—O11^{ii}	51.8 (2)
O5^{iv}—K2—O4^{iii}	143.49 (9)	O3^{xi}—K4—O11	142.8 (4)
O5^{iv}—K2—O6^{v}	136.32 (8)	O3^{xi}—K4—O11^{ii}	105.0 (4)
O5^{iv}—K2—O10	72.03 (7)	O3^{xi}—K4—O14S^{xii}	78.7 (3)
O5^{iv}—K2—O14S	73.66 (10)	O7—K4—Mo3^{ii}	94.4 (3)
O5^{iv}—K2—O15S^{vi}	77.67 (9)	O7—K4—Mo3	27.22 (12)
O6^{v}—K2—Mo1	155.66 (7)	O7—K4—O2^{ii}	87.35 (18)
O6^{v}—K2—Mo2	105.79 (6)	O7—K4—O3^{ii}	119.2 (4)
O6^{v}—K2—K1	108.31 (6)	O7—K4—O9^{i}	55.3 (2)
O6^{v}—K2—O1	153.12 (8)	O7—K4—O11	54.6 (2)
O6^{v}—K2—O2	95.19 (8)	O7—K4—O11^{ii}	67.7 (2)
O6^{v}—K2—O4^{iii}	67.03 (8)	O7—K4—O14S^{xii}	103.4 (4)
O6^{v}—K2—O10	129.77 (8)	O9^{i}—K4—Mo3^{ii}	132.2 (4)
O6^{v}—K2—O15S^{vi}	83.98 (9)	O9^{i}—K4—Mo3	39.02 (15)
O7^{vi}—K2—Mo1	125.19 (6)	O9^{i}—K4—O2^{ii}	138.7 (3)
O7^{vi}—K2—Mo2	143.61 (7)	O9^{i}—K4—O3^{ii}	151.0 (4)
O7^{vi}—K2—K1	152.55 (7)	O9^{i}—K4—O11^{ii}	117.1 (4)
O7^{vi}—K2—O1	129.86 (8)	O9^{i}—K4—O14S^{xii}	62.7 (3)
O7^{vi}—K2—O2	161.39 (9)	O11^{ii}—K4—Mo3^{ii}	29.26 (12)
O7^{vi}—K2—O4^{iii}	118.29 (8)	O11—K4—Mo3^{ii}	77.1 (3)
O7^{vi}—K2—O5^{iv}	63.61 (8)	O11—K4—Mo3	31.51 (13)
O7^{vi}—K2—O6^{v}	73.99 (8)	O11^{ii}—K4—Mo3	78.1 (2)
O7^{vi}—K2—O10	123.76 (8)	O11—K4—O2^{ii}	119.4 (3)
O7^{vi}—K2—O14S	72.25 (10)	O11^{ii}—K4—O2^{ii}	49.33 (15)
O7^{vi}—K2—O15S^{vi}	77.89 (9)	O11—K4—O3^{ii}	97.1 (4)
O10—K2—Mo1	29.34 (4)	O11—K4—O9^{i}	55.4 (2)
O10—K2—Mo2	30.28 (4)	O11—K4—O11^{ii}	71.7 (3)
O10—K2—K1	76.74 (5)	O11—K4—O14S^{xii}	115.3 (4)
O14S—K2—Mo1	97.10 (9)	O14S^{xii}—K4—Mo3	100.2 (3)
O14S—K2—Mo2	139.00 (9)	O14S^{xii}—K4—Mo3^{ii}	162.1 (4)
O14S—K2—K1	80.82 (8)	O14S^{xii}—K4—O2^{ii}	118.6 (4)
O14S—K2—O1	77.14 (10)	O14S^{xii}—K4—O3^{ii}	136.6 (4)
O14S—K2—O2	125.79 (10)	O14S^{xii}—K4—O11^{ii}	163.5 (3)
O14S—K2—O4^{iii}	72.99 (9)	O15S—K4—Mo3^{ii}	115.5 (3)

O14S—K2—O6^{v}	103.78 (11)	O15S—K4—Mo3	100.4 (3)
O14S—K2—O10	126.00 (10)	O15S—K4—O2^{ii}	56.71 (18)
O14S—K2—O15S^{vi}	145.39 (11)	O15S—K4—O3^{xi}	85.9 (4)
O15S^{vi}—K2—Mo1	85.92 (7)	O15S—K4—O3^{ii}	112.7 (4)
O15S^{vi}—K2—Mo2	66.07 (7)	O15S—K4—O7	76.9 (3)
O15S^{vi}—K2—K1	129.36 (8)	O15S—K4—O9^{i}	94.4 (4)
O15S^{vi}—K2—O1	110.82 (9)	O15S—K4—O11^{ii}	96.8 (2)
O15S^{vi}—K2—O4^{iii}	138.64 (9)	O15S—K4—O11	131.2 (4)
O15S^{vi}—K2—O10	59.81 (8)	O15S—K4—O14S^{xii}	67.2 (3)
Mo1—O1—K1	127.60 (13)	O15S—K4—O16S	154.6 (5)
Mo1—O1—K2	108.13 (12)	O16S—K4—Mo3	100.0 (4)
K1—O1—K2	84.23 (7)	O16S—K4—O7	126.0 (5)
Mo2—O2—K1	129.18 (12)	O16S—K4—O11	71.7 (4)
Mo2—O2—K2	112.55 (12)	K4^{ix}—O16S—K4	108.9 (10)

Symmetry codes: (i) −*x*+3/2, −*y*+1/2, −*z*+2; (ii) −*x*+1, −*y*, −*z*+2; (iii) −*x*+1, *y*, −*z*+3/2; (iv) −*x*+1, −*y*+1, −*z*+2; (v) −*x*+1/2, −*y*+1/2, −*z*+2; (vi) *x*−1/2, *y*+1/2, *z*; (vii) *x*, −*y*, *z*−1/2; (viii) *x*−1/2, −*y*+1/2, *z*−1/2; (ix) −*x*+1, *y*, −*z*+5/2; (x) *x*+1/2, *y*−1/2, *z*; (xi) *x*, −*y*, *z*+1/2; (xii) *x*+1/2, −*y*+1/2, *z*+1/2.